Anodic process on Cu-Al Alloy in KF-AlF_3-Al_2O_3 melts and suspensions

Sai Krishna Padamata*, Andrey S. Yasinskiy, Petr V. Polyakov
School of non-ferrous metals and materials science, Siberian federal university, Krasnoyarsk, Russia
*Corresponding author id: saikrishnapadamata17@gmail.com

Abstract

Inert anode development has been a topic of interest for decades. Cu-Al, Fe-Ni based alloys have shown promising results in low-temperature melts. Metallic anodes tend to contaminate the produced aluminium with their corrosion products and introducing alumina suspension particles in the electrolyte could resolve this problem by suppressing the convective transfer of corrosion products toward aluminium produced. In this paper, anodic processes on Cu-10Al electrode in molten KF-AlF_3-Al_2O_3 (5 wt. %) and suspensions were characterized. Effects of cryolite ratio CR $\left(\frac{Mole\ \%\ KF}{Mole\ \%\ AlF_3}\right)$, temperature and particle volume fraction (φ= 0 – 0.15) on the electrochemical behaviour of the anode were demonstrated. The results suggest that CR = 1.4 at 800 °C with the particle volume fraction of not more than 0.09 are better parameters for the usage of Cu- 10Al anode. At melts with φ= 0.15 at all temperatures and CR values, a low current density was observed.

Keywords: *aluminium, suspension, oxidation, inert anode, cryolite melt, low-temperature electrolysis*

Introduction

Production of aluminium is carried out by aluminium oxide decomposition in the molten sodium cryolite at an industrial scale by using Hall-Heroult cell. The process is been in use for more than 100 years with periodic upgrades. Carbon is used as an anode where CO_2 evolution takes place, leading to the consumption of anodes on a regular basis enforcing the periodic replacement of anodes. Other than CO_2, greenhouse gases like CO, COF_2, CF_4, and C_2F_6 are also emitted. The following reactions occur in the process of aluminium reduction:

$$Al_2O_{3(dis)} + 3/2C_{(s)} \overset{6F}{\Rightarrow} 2Al_{(l)} + 3/2CO_{2(g)} \quad (1)$$

with (EMF) $E^0 = 1.168$V at 1000 °C

$$Al_2O_{3(dis)} + 3C_{(s)} \overset{6F}{\Rightarrow} 2Al_{(l)} + 3CO_{(g)} \quad (2)$$

with $E^0 = 1.033$V,

$$4AlF_{3(dis)} + 3C_{(s)} \overset{12F}{\Longrightarrow} 4Al_{(l)} + 3CF_{4(g)} \quad (3)$$

with $E^0 = 2.155$V and,

$$2AlF_{3(dis)} + 2C_{(s)} \overset{6F}{\Rightarrow} 2Al_{(l)} + C_2F_{6(g)} \quad (4)$$

with $E^0 = 2.378$V.

This scenario can be avoided by introducing inert anode to the process, which not only eliminates the emission of greenhouse gases, but also the cost associated with the fabrication of the carbon anodes. Inert anodes have been the centre of interest for researchers for a while and attempts are made to find suitable materials to replace existing carbon anode. Oxygen is evolved at the inert anodes and the reaction (5) takes place.

$$Al_2O_{3(dis)} \overset{6F}{\Rightarrow} 2Al_{(l)} + 3/2O_{2(g)} \quad (5)$$

with $E^0 = 2.337$V at 750 °C.

A material should meet the following requirements to qualify as an inert anode: (1) good electrical conductivity, (2) low corrosion rate, (3) high stability at high-temperature electrolysis, (4) easy fabrication and low maintenance [1, 2]. The energy balance and environmental challenges using inert anodes were discussed extensively earlier [3] [4]. Metallic, ceramic and cermet materials were

tested to date and each has its advantages and disadvantages [5-12]. Metallic anodes have been showing promising results, as they possess high electrical conductivity, good thermal shock resistance. Moreover, the scales formed on the surface of the anode protects it from the oxidation.

During the electrolysis process, the oxide layers are formed on the surface of the metallic anode. If the oxide layer shows good conductivity and stable microstructure while adhering well with the anodic material then it can be considered as a good candidate for anodic material. However, in most cases, the oxide layers react with the cryolite, which results in corrosion. Reaction (6) would occur when the oxide scale reacts with the molten cryolite.

$$M_xO_y + \frac{2y}{3}Na_3AlF_6 = M_xF_{2y} + \frac{y}{3}Al_2O_3 + 2yNaF \quad (6)$$

The performance of an anode depends upon the electrolyte used and it is advantageous to use melts with low liquidus temperature while using metallic inert anodes to minimize the corrosion. Extensive studies have been carried out on sodium and potassium cryolites. The aluminium electrolysis process is carried out at around 960 °C using NaF_3-AlF_3 melt but while using the KF-AlF_3 melts, the process can be performed at 700-800 °C. Low-temperature melts are highly desirable as inert anodes possess low corrosion rate and thermal shocks at these conditions[13-21]. Nevertheless, decreasing the electrolyte temperature leads to an increase in the decomposition voltage by 0.10–0.15V. Selection of Cu-Al alloy as an anode for the present study in the melts and suspensions was based on the following properties possessed by the alloy [22, 23]:

- melting point of the anode is around 1050 °C which allows electrolyte overheating;
- relatively high electrical conductivity of the alloy and its oxide scale (copper oxide and copper aluminates) formed during the electrochemical process;
- stability of the copper aluminates in fluoride melts saturated by the oxygen ions;
- high corrosion resistance at 750 °C in KF-AlF_3 melts with cryolite ratio CR $\left(\frac{Mole\,\%\,KF}{Mole\,\%\,AlF_3}\right)$ = 1.3-1.8.

Suspension melts have also been suggested for the aluminium electrolysis process. The particles should be evenly dispersed with no sedimentation. Zero sedimentation of alumina was obtained at a volume fraction of 0.32 [24]. This type of melt increases the purity of the produced liquid aluminium by stopping the corrosion products from contacting it and resolve the problem of maintaining the electrolyte saturated with alumina [25, 26]. Although, an increase in the volume fraction of alumina results in the increased electrical resistance of the suspension. Although, this issue can be minimized by decreasing the anode-cathode distance.

In the previous work [27, 28], three anodic materials with the compositions Cu – 9Al – 5Fe, Cu – 10Al and Cu – 10Al – 1.7Be were investigated at 750 °C with KF-AlF_3-Al_2O_3 at CR=1.3. Results suggested that Cu – 10Al was performing better out of the three at given conditions and further research must be conducted to explore its performance at different temperatures in different melts and suspensions. Reactions shown in table 1 occur on Cu- 10Al electrode during the oxidation process and the sum of half-reactions of the oxidation-reduction which correspond to the Gibbs energies and are associated with the potential difference (EMF) as shown:

$$E^0 = -\frac{\Delta G^0}{z \cdot F} \quad (7)$$

where z is the number of electrons, $F = 96585$ [C/mol] is the Faraday constant.

Table1. Possible reactions occurring on Cu – 10 Al anode at 750 °C per 1 mole of Al.

Reaction		ΔG^0_{1023K}, kJ/mol	ΔH^0_{1023K}, kJ/mol	ΔS^0_{1023K}, kJ/mol·K	E^0, V
$Al_2O_{3(dis)} + 3Cu_{(s)} \overset{6F}{\Rightarrow} 2Al_{(l)} + 3CuO_{(s)}$	(8)	580.21	621.63	40.48	2.00
$Al_2O_{3(dis)} + 6Cu_{(s)} \overset{6F}{\Rightarrow} 2Al_{(l)} + 3Cu_2O_{(s)}$	(9)	535.79	595.54	58.40	1.85
$2Al_2O_{3(dis)} + 3Cu_{(s)} \overset{3F}{\Rightarrow} 1.5Cu_2Al_2O_{4(s)} + Al_{(l)}$	(10)	513.90	58.44	44.19	1.78
$2Al_2O_{3(dis)} + 1.5Cu_{(s)} \overset{3F}{\Rightarrow} 1.5CuAl_2O_{4(s)} + Al_{(l)}$	(11)	393.77	453.57	58.44	1.36

Note: The calculations were carried out in the HSC Chemistry v.9.6.1 software

The present study aims to determine the electrochemical behaviour of Cu – 10Al anode in $KF\text{-}AlF_3\text{-}Al_2O_3$ melts and suspensions. The anode was tested with melt (CR = 1.3) at 750 °C with varying particle volume fraction (φ = 0 to 0.15). Ultra-fine alumina particles were used to minimize the sedimentation. CR values and temperatures were varied in the range of 1.2-1.5 and 700–850 °C respectively. This article presents the results of the galvanostatic polarization and cyclic potentiometry studies performed.

Experimental

Material preparation and characterisation

Alloy with a composition of Cu- 10 Al (in wt. %) was prepared in a vacuum melting furnace at 1050 °C. The materials used for the preparation had a purity of Cu (99.95 %) and Al (99.999%). The equilibrium phase of the Cu-Al system was fcc ($\propto$ Cu-Al) solid solution [29]. The specimens were cut in a cylindrical shape with dimension ϕ 15mm × 50 mm. The specimens were treated with degreasing agents (acetone and ethanol) and then dried in the air before the usage. A hole with ϕ2.5mm was drilled and threading was made to assemble current lead (steel rod) with the anode. The unused anodic part and the steel current lead were protected with a BN tube insulator.

Electrolytes with CR between 1.2 and 1.5 were synthesized. Firstly, a crystalline form of KF was heated in the vertical furnace to remove the water present in the salt at 400 °C for 4 hours. While synthesizing the electrolyte, the AlF_3 salt was placed at the bottom of the crucible and the KF salt was set at the top as AlF_3 tends to sublimate quickly at 800 °C and higher. The synthesis process was carried out for 3 hours. The melt was mixed well and a portion of alumina was added corresponding to its saturation point in the melt (5 wt.%) with continuous stirring. The temperature during the preparation of melt was monitored throughout the process with the help of a k-thermocouple protected with BN sleeve, which was immersed in the electrolyte. The melt was transferred to a container where it was left to solidification. The solidified melt was then crushed and used accordingly. All the chemicals used were analytical grade and alumina used has an average particle size less than 5µm as shown in Fig. 1.

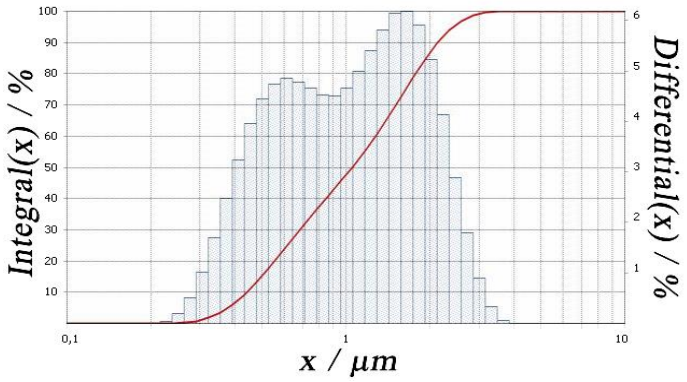

Fig. 1. The particle size distribution of Al_2O_3

Cell design and experimental method

The three-electrode cell as shown in Fig. 2 was used to perform the experiments. Graphite crucible with high purity was used to contain $KF\text{-}AlF_3\text{-}Al_2O_3$ (5wt. %) melt. The crucible also acted as a counter electrode. The reference electrode Al/AlF_3 was used which connected to the measuring device using tungsten rod. The reference electrode setup had a porous BN tube containing the liquid aluminium and $KF\text{-}AlF_3$ electrolyte.

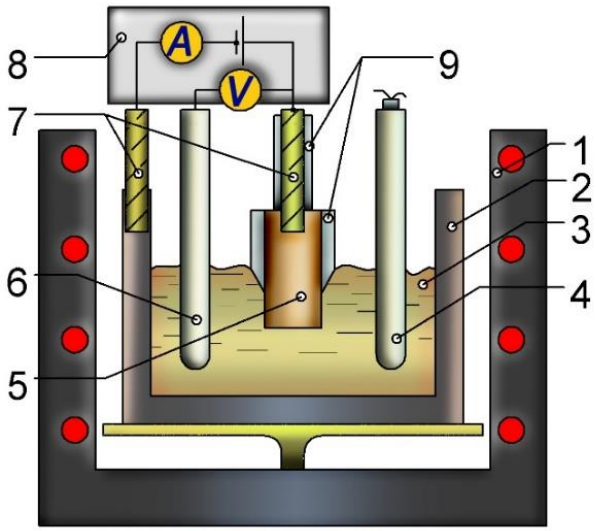

Fig. 2. *Experimental setup: 1 - Furnace; 2 - graphite crucible h = 110 mm, d_{int} = 76 mm, d_{ext} = 92 mm; 3 – electrolyte/suspension KF-AlF_3-Al_2O_3; 4 - thermocouple; 5 - anode sampled = 15 mm, h = 10 mm; 6 - reference electrode (Al/AlF_3); 7 - steel current leads, 8 – potentiostat, 9 – BN shields*

Autolab PGSTAT302n potentiostat equipped with a 20A booster and controlled by NOVA 2.1.2 software was used to carry out the electrolysis. Electrolysis was conducted using chrono potentiometric method according to which the stable potential was obtained and a relatively stable oxide layer was formed on the anodic surface. Stationary polarization was performed for 0.005 to 1.5 A/cm^2 current densities where the recording was made with 30 µs of current interruption after a 120s current passage to determine the ohmic voltage drop (IR). Cyclic voltammetry was performed at 0.05 V/s scan rate to examine the possible anodic reactions. The anodic overvoltage was calculated according to the equation:

$$\eta_a + \eta_c = E_i - E_r - IR \quad (12)$$

where η_a is the activation overvoltage, η_c is the concentration overvoltage, E_i is the potential difference between the anode under current and the reference electrode, E_r is the anodic reversible potential relative to the reference electrode, I is the current, R is the resistance. The activation and concentration overvoltages were not divided, and the sum was treated as total anodic overvoltage in this paper.

Results and Discussion

Oxide layer characterisation

Initially, anodes were polarized in melts (CR = 1.3) and suspensions (φ = 0.12) for 1 to 1.5 hours at 750 °C with the current density i=0.4 A/cm^2 to record the change of total voltage being supposedly associated with the oxide layer formation vs. time as shown in Fig. 3

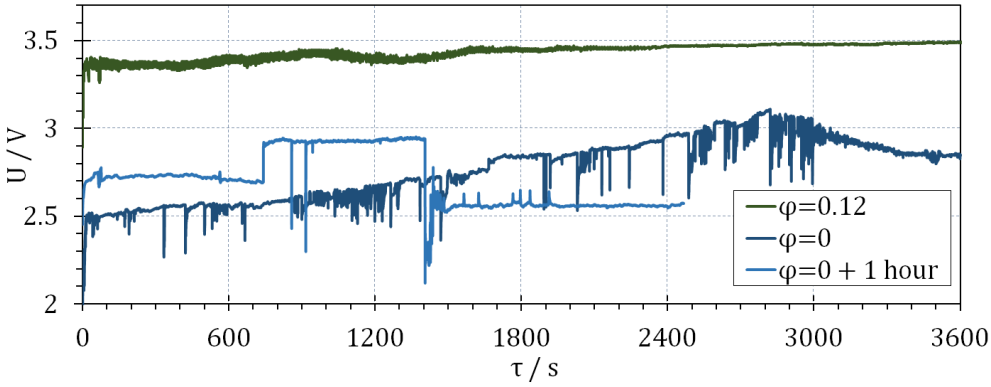

Fig. 3. *Galvanostatic polarization CR=1.3 750 at 0.4 A/cm^2*

Stationary anodic polarization in melt changed between 2.5 V and 3.1 V. The anodic potential was increased from 2V (open circuit potential) up to 3.1 V. Consistent change in the anodic potential reflects the formation of different types of oxide layers (copper oxides and copper aluminates) and changes in its structure. High oscillations of the anodic potential might be associated with the formation of new oxide layer on a consistent basis or due to the bubble evolution on the anodic surface leading to the reduction of the active surface area. No stable oxide layer was formed even after an hour of polarization. The stable oxide layer was formed after 5000 seconds of polarization. In case of anodic polarization in suspension (φ = 0.12), a stable oxide layer was formed from the beginning of the polarization and only a minor shift of anodic potential was observed. No fluctuations in the voltage were seen unlike anode tested in melt. The sedimentation was not observed.

The XRD results from Fig. 4 and Table 2 show the composition of oxide layers formed on the anode during the polarization.

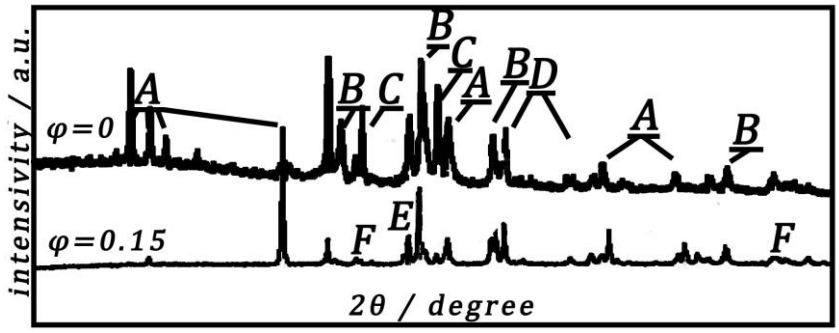

Fig. 4. *XRD-graphs recorded on oxide layers after anodic polarization in melts and in suspensions with φ = 0.15 at 750 °C: A) electrolyte phases, B) Cu_2O, C) $CuAlO_2$, D) Cu, E) $CuAl_2O_4$, F) CuO*

Table 2. Oxide layer composition after polarization in melt and suspension (wt.%)

φ	CuO	Cu_2O	$CuAlO_2$	$CuAl_2O_4$
0.00	0	30.34	53.63	16.03
0.15	31.16	42.84	11.77	14.22

No CuO oxide layer was observed from XRD results and the dominant oxide layer in terms of proportion was $CuAlO_2$ for melts (φ=0), while in suspensions (φ= 0.15) the most dominant oxide layer on the surface of the anode was Cu_2O, while $CuAlO_2$ content was low unlike in melts (φ=0). No CuF or CuF_2 was found on XRD examinations meaning CuF and CuF_2 produced from the process are dissolved in the electrolyte. The anodes were tested with stationary and non-stationary methods in melts (φ=0) and suspensions ($0.03 \leq \varphi \leq 0.15$) at different temperatures and CR to find the best conditions at which the anode can perform.

Effect of temperature and CR

To characterize the effect of temperature and CR on the anodic behaviour of Cu – 10Al alloy both stationary and non-stationary polarization techniques were applied. Cyclic voltammetry was performed on anodes at 700 and 800 °C in melts saturated with alumina at CR = 1.2 – 1.5. Voltammograms recorded to observe the response of anode with the change in potential at 0.05 V/s scan rate are illustrated in the Fig. 5.

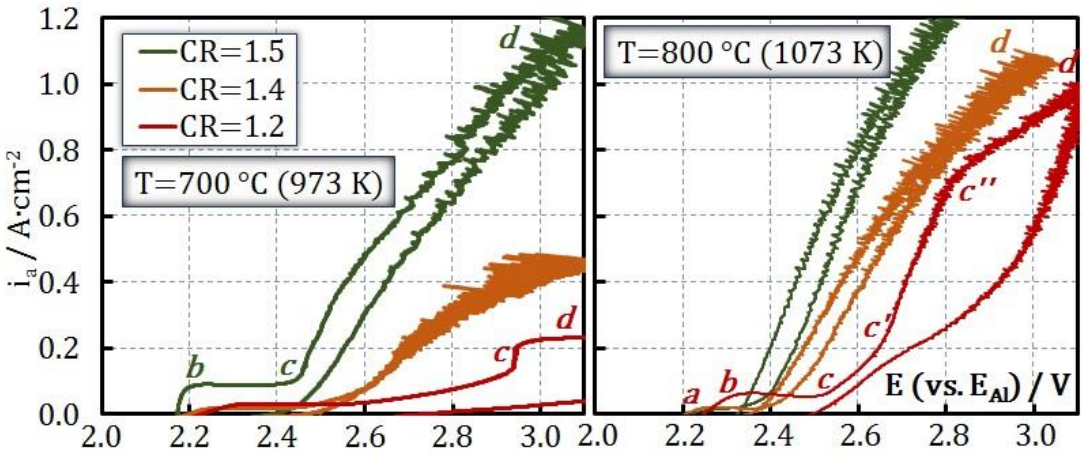

Fig. 5. *Cyclic voltammograms for the anode in melts with different CR (1.2-1.5) at 700 and 800 °C*

Several regions can be distinguished on the curves. The ***ab*** region between 2.1 and 2.3 V is where the metal oxidation takes place. After that, a region ***bc*** with a plateau or a slight decrease in current with the potential shift toward more positive values can be observed. In [30] similar regions were indicated as the passivation of the anode. The transpassivation process of the anode takes place in the region ***cd*** where the oxygen starts to evolve. The current density fluctuation at potentials after 2.5 V is due to the bubbles evolution on the anode surface leading to the constant change in the active anode surface and the interpolar resistance. No passivation of the anode was observed at 800 °C for CR = 1.4 and CR = 1.5. With the decrease in the CR, reduction of anodic current density at the particular anodic potentials (in oxygen region ***cd***) can be seen.

For melts with CR 1.2 at 700 °C, current density remains low, indicating the passivation of the anode from the beginning of the process. After increase in the temperature to 800 °C the shape of the curve in the oxygen region had changed. The region ***c'c''*** appeared where the $\partial i/\partial E$ value was higher than that of ***cc'*** and ***c''d*** regions. The reason might be associated with change in resistance during the sweep due to passivation and transpassivation phenomena. High current densities were achieved while using melts with CR =1.5. This can be related to higher alumina solubility in melt at higher CR.

The reversible potentials and the stationary potentials at i=0.4 A cm^{-2} obtained through the galvanostatic process for 1.2≤CR≤1.5 are illustrated in Fig. 6. An increase in the CR results in the decrease of the anodic potential and evolution of oxygen at low current densities. The reason is that an increase in AlF_3 concentration in the melts leads to the formation of oxyfluoroaluminates like $AlOF_x^{1-x}$,$Al_2OF_x^{4-x}$,$Al_2O_2F_x^{2-x}$, Al_4OF_8, Al_4OF_{10} at higher rates leading to the difficulties in the ions transport between the anode and the cathode [32,33].

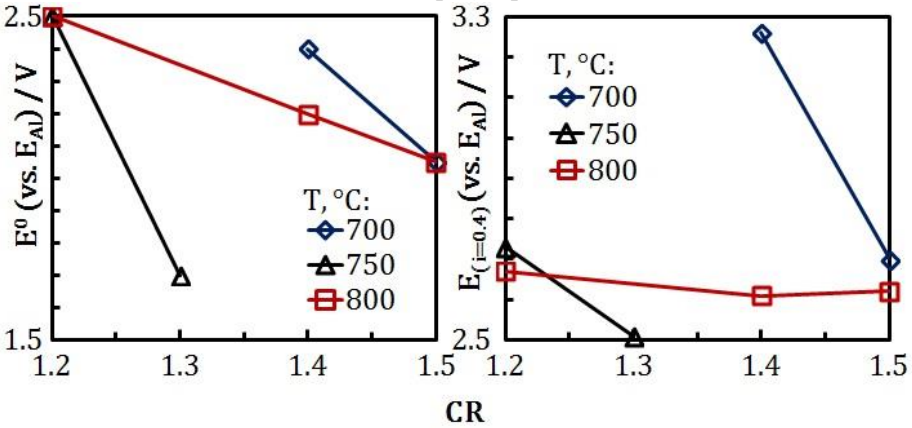

Fig. 6. *Dependence between reversible potential (left) and stationary potential at 0.4 A/cm^2 (right) in melts at 700, 750 and 800 °C vs. CR*

In case of melts with CR = 1.5, the effect of temperature on the anodic potential was not observed until the oxygen evolution potential (2.34V). The limiting current densities were observed at high potentials (3.2-4.2 V) for CR = 1.2 at both the temperatures. In case of CR= 1.4, limiting currents were in the region from the potential 2.9V. At CR = 1.5, the limiting current region is between the potentials (3.4 -4.2V) in melts at 700 °C and no limiting currents were observed at 800 °C. In melts with CR= 1.4, drastic variation in current density w.r.t anodic potential was seen with the change in temperature.

According to the obtained results, the anode performed better at 800 °C. A further increase in temperature is undesirable due to probable decrease in corrosion resistance. The CR should be maintained at CR≈1.4. The reasons for the chosen parameters are:

- the onset potential of oxygen evolution is more negative at higher temperatures and higher CR;
- high overvoltage is observed at temperatures below 800 °C;
- the stationary anodic potentials at current density 0.4 A cm^{-2} were similar in melts with CR=1.4 and CR=1.5;
- in terms of the cathodic process the lower CR is preferable due to higher limiting currents of aluminium reduction [31], so the optimal CR value can be between 1.3 and 1.4.

Effect of particles volume fraction

Stationary galvanostatic polarization curves were recorded for melts (φ=0) and suspension (φ=0.03…0.15) under chosen conditions (T=800 °C, CR=1.4) to estimate the limiting current density and the effect of particle volume fraction on the polarization curve. The data was compared to the previously obtained results for initially chosen conditions (T=750 °C, CR=1.3). The plots are shown in the Fig. 7 [27].

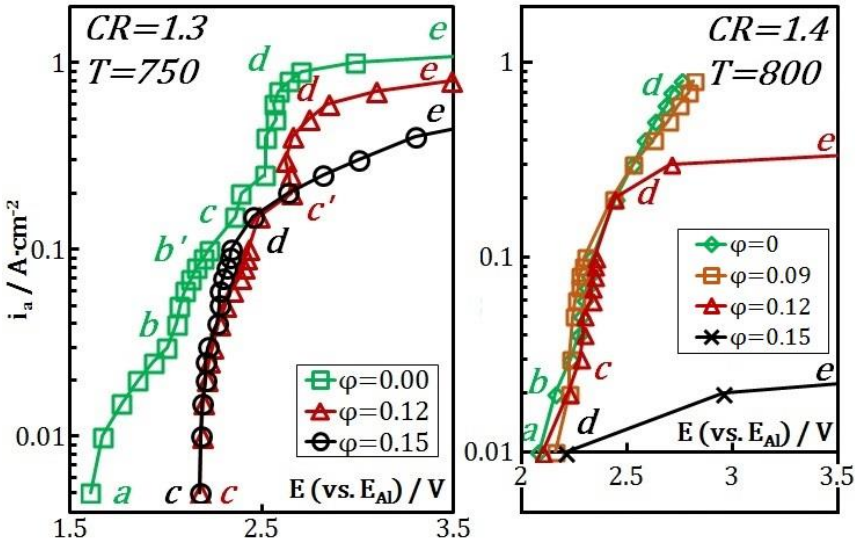

Fig. 7. *Stationary galvanostatic polarization curves of the anodic process in melts and suspensions (φ=0-0.15) with CR 1.3 and 1.4 at 750 °C and 800 °C*

The metal oxidation takes place in the region ***ab***. The potentials in melt (φ=0) with CR=1.3 indicate the formation of copper aluminates rather than oxides (see Table 1). At point ***b***, the potential was equal to that of the Cu/CuO electrode, which shows the formation of CuO layer on the electrode in the region ***bc***. Point ***c*** is where the oxygen evolution starts and it can be seen that the oxygen evolution takes place at high i in the melts (φ=0) and starts at low i while using suspensions. A sharp increase in the current density indicating the oxygen evolution onset can be seen in the regions ***cd*** and ***c'd*** in suspension. The electrode in suspensions at φ=0.15 had no metal oxidation region ***ab***.

The limiting current densities were observed in the ***de*** region. It is observed that the electrode used in melts (φ=0) possess high limiting current density while an increase in φ drops the limiting

currents, which might be due to the decrease in mass transfer coefficient K_s of the oxyfluoride ions. States that with increasing suspension volume fraction in melts, limiting current decreases.

The comparison of the described results with those obtained in suspensions with CR 1.4 at 800 °C allows us to conclude that the limiting currents can be observed at 2.5-3 V in the suspension with φ= 0.12–0.15. In case of suspensions with lower φ (0.09) and melts, limiting current densities were not achieved up to 1 A cm^{-2}. With an increase in the volume fraction φ from 0.12 to 0.15, the passivation of the anode was observed. From the galvanostatic curves, it can be concluded that the volume fraction with no more than 0.09 can be used. Further increase in the φ leads to drastic increase in overvoltage.

The cyclic voltammetry recordings were made at a scan rate of 0.05 V/s in suspensions (φ=0.03–0.15) at 800 °C and compared to those obtained previously [27] as shown in the Fig. 8.

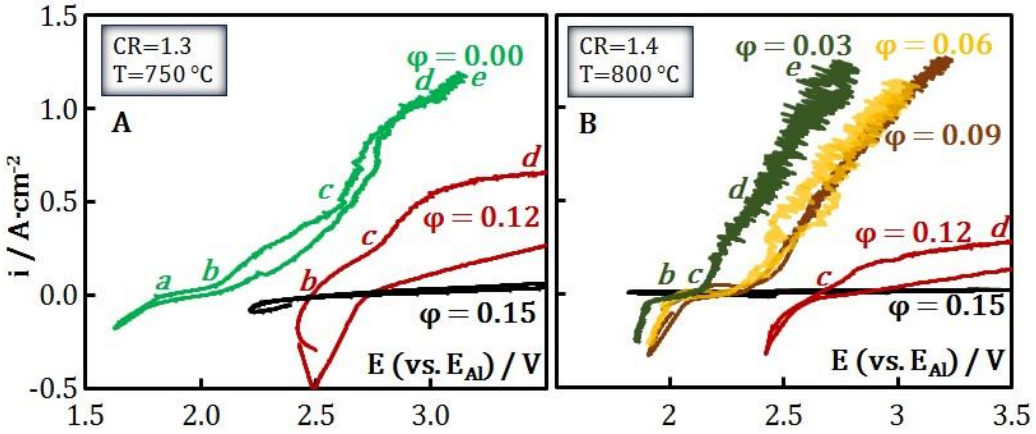

Fig. 8. Cyclic voltammograms recorded in melts suspension with CR 1.3 and 1.4 at 750 °C and 800 °C

In case of pure melts, low current densities were observed, reflecting metal oxidation stage in the regions ***ab*** and ***bc***. The potential at point ***b*** was 2.07 V, which is closer to the potential corresponding to Cu/CuO electrode (2.00 V). CuO might have been a dominating oxide layer on the surface of the electrode in the ***bc*** region while before that rather copper aluminates or Cu_2O were formed. Oxygen evolution happens from point ***c*** where the potential of the anode was above 2.5 V in the melt with CR=1.3. It has shifted toward more negative value after increase in CR. Point ***c*** separates the pre-oxygen and oxygen evolution regions. At the region ***de***, an increase in the current density can be seen and reason might be due to the reaction (13). In suspensions with high φ (0.12 and 0.15) at point ***c***, the potential is more than 2.6V, which is close to the EMF of the reaction (14). The active CuO layer oxidation may take place leading to the formation of CuF_2 and O_2 evolution and it states the catastrophic corrosion of an oxide layer.

$$AlF_{3(l)} + Cu_{(s)} \overset{3F}{\Rightarrow} CuF_{2(s)} + Al_{(l)} \quad (13)$$

with $E^0 = 2.31$ V

$$\frac{4}{3}AlF_{3(l)} + 2CuO_{(s)} \overset{4F}{\Rightarrow} 2CuF_{2(s)} + \frac{4}{3}Al_{(l)} + O_{2(g)} \quad (14)$$

with $E^0 = 2.65$ V

In suspensions with φ = 0.12, oxygen evolution takes place from the beginning at 2.45V and reaction (15) is expected which occurs at potential 2.29 V, readily formed $Cu_2Al_2O_4$ oxide on the anodic surface at the beginning of the voltammetry process is transformed to CuO and oxygen evolution takes place at the same time. In the regions ***cd*** and ***de***, the dissolution of the CuO oxide layer takes place with continuous O_2 evolution at potentials close to those required for the reaction (14) where CuO layer reacts with the AlF_3 present in the electrolyte and CuF is expected to be the product along with $Al_{(l)}$ and evolution of O_2.

$$1.5Cu_2Al_2O_4 + Al_2O_3 \overset{4F}{\Rightarrow} 3CuO + 5Al_{(l)} + 3O_{2(g)} \quad (15)$$

with $E^0 = 2.29$ V

In the ***cd*** region, passivation of the anode may takes place where the reason might be the formation of the specific oxyfluoroaluminates. In suspensions with φ = 0.15, since the beginning of the sweep, high resistance was observed and no reactions occurred with considerable rate. The anode surface was completely passivated.

The dependence between the stationary current density at 2.7 V and the φ for suspension with CR=1.4 at 800 °C is shown in Fig. 9.

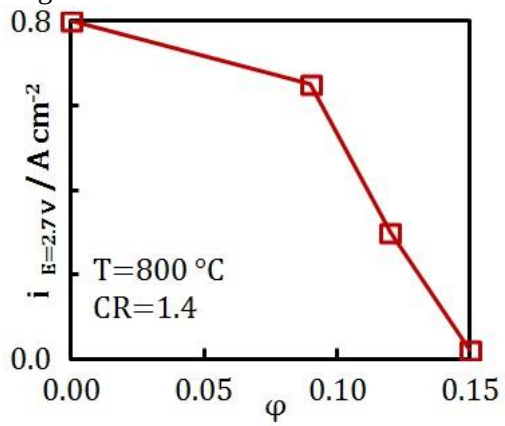

Fig. 9. Dependence between stationary current density i at anodic potential E=2.7 V (relative to Al reference electrode) and alumina particles volume fraction in suspension with CR=1.4 at 800 °C

It can be observed that the stationary current slightly decreases in the range of φ between 0 and 0.09. After the introduction of additional alumina particles, the limiting current of oxygen evolution seems to be decreased. As a result the observed stationary current decreases rapidly with increase in φ. Equation (16) represents the mass transfer coefficient correlated with the limiting current and solubility of alumina [34]:

$$k_s = \frac{i_l}{zFC} \quad (16)$$

where k_s [cm/s] is the mass transfer coefficient, z is the number of electrons, i_l [A/cm^2] is the limiting current density, F= 96500 [C/mol] is the Faraday's constant, C [mol/cc] is the solubility. The mass transfer coefficients are calculated for the set of conditions and presented in Table **3**.

Table 4. Mass transfer coefficients for diffusion of electroactive particles to the anode

T/ °C	CR	φ	i_l/A·cm^{-2}	C/ mol·cc^{-1}	k_s·10^4/ cm.s^{-1}
750	1.3	0	0.90	0.00901 [35]	5.175
750	1.3	0.12	0.60	0.00901 [35]	3.450
750	1.3	0.15	0.15	0.00901 [35]	0.862
800	1.4	0.03	1.10	0.00738 [36]	7.722
800	1.4	0.12	0.20	0.00738 [36]	1.404
800	1.4	0.15	0.02	0.00738 [36]	0.140

Clearly, k_s value decreases with the increasing volume fraction in both cases; although the k_s values decrease with the increase in CR. The limiting currents for CR 1.4 at low φ were not observed resulting in the difficulties to estimate k_s. It is worth noting that k_s slightly decreases with an increase in φ if φ≤0.12. However, any further increase in φ leads to the drastic drop of k_s. The obtained $\boldsymbol{k_s}$ values are relatively less compared to the values obtained for gas evolving electrodes [37,38].

The industrial process of aluminium reduction in alumina suspensions seems to be operable with φ≈0.09 if the highly dispersed alumina is used.

Conclusion

The influence of dispersed alumina particles content in melts on the current-potential characteristics is discussed. The main conclusions:

- The dominant oxide layer on the anode surface in melts (φ=0) was $CuAlO_2$ and while using suspension (φ=0.15) Cu_2O was the dominant one;

- with the increase in the alumina volume fraction, the limiting current densities of metal oxidation and oxygen evolution decrease;
- passivation of the anode at the beginning of the cyclic voltammetry process was seen at 700 °C at all CR values (1.2-1.5). The reasons might be the oxide formation or the reduction in the anodic active surface area;
- particle volume fraction (φ) of 0.09 is suggested for the further process development;
- anode possesses high oxygen evolution limiting currents at 800 °C.

Further work will be conducted to analyze the current efficiency with Cu-10Al alloy at 800 °C in suspension with φ = 0.09 and CR=1.4.

Acknowledgments

The reported study was funded by Russian Foundation for Basic Research, Government of Krasnoyarsk Territory, Krasnoyarsk Region Science and Technology Support Fund according to the research project № 18-48-243014.

References

1. Galasiu I., Galasiu R., Thonstad J., "Inert Anodes for Aluminium Electrolysis", Aluminium-Verlag, 2007, Diisseldorf, 207 p
2. Pawlek R.P., "Inert anodes: an update", Light Metals, 2014, 1309-1313
3. Kvande H., and Haupin W. "Inert anodes for aluminium smelting: energy balances and environmental impact", JOM 2001, 53 (5), 29-33.
4. Sadoway D.R., "Inert anodes for the Hall-Heroult cell: the ultimate materials challenge", JOM 2001. 53(5), 34-35.
5. Liu Jian-Yuan, Li Zhi-You, Tao Yu-Qiang, Zhang Dou, Zhou Ke-Chao., "Phase evolution of 17(Cu-10Ni)-(NiFe2O4 – 10NiO) cermet inert anode during aluminium electrolysis", Transaction of Non-ferrous metals in China, 2011, 21 (3), 566-572.
6. Glucina M., Hyland M., "Laboratory scale testing of Aluminium Bronze as an inert anode for Aluminium Electrolysis", Light Metals, 2005, 523-528.
7. Nguyen Th., de Nora V., "de Nora Oxygen evolving inert metallic anode", Light Metals, 2006, 385-390.
8. Helle S., Pedron M., Assouli B., Davis B., Guay D., Roue L., "Structure and high temperature oxidation behaviour of Cu-Ni-Fe based alloys prepared by high-energy ball milling for application as inert anodes for aluminium electrolysis", Corrosion Science, 2010,52(10), 3348-3355.
9. Helle S., Tresse M., Guay D., Roue L., "Mechanically alloyed Cu-Ni-Fe-O based materials as oxygen evolving anodes for aluminium electrolysis", Journal of Electrochemical society, 2012, 159(4), 62-68.
10. Gavrilova E., Goupil G., Davis B., Guay D., Roue L., "Influence of Partial substitution of Cu by various elements in Cu-Ni-Fe alloys on their high temperature oxidation behaviour", Light Metals, 2015, 1187-1191.
11. Zaikov Yu.P. "Ceramic properties of electrodes based on NiO-Li_2O and their solubility in cryolite alumina melts", VIII. Al Sympozium, 25-27 Sept. 1995. Slovakia, Ziar nad Hronom-Donovaly, 239-241.
12. Haarberg G.M. "The interaction between tin oxide and cryolite-alumina melts", 9th Int. Symp. On Molten Salts, San Francisco, USA, 22-27 May 1994, 568-577.
13. Nguyen Q.M., "Extraction of Metals by Molten Salt Electrolysis: Chemical Fundamentals and Design Factors", JOM, January, 1985, 28-33.
14. Grjotheim K., Malinovsky M., and Matiasovsky K., "The Effect of Different Additives on the Conductivity of Cryolite-Alumina Melts", JOM, January 1969, 29-33.
15. Solheim A., Rolseth S., Skybakmoen E., Stoen L., "Liquidus Temperature and Alumina Solubility in the System Na3AlF6-AIF3-LiF-CaF2-MgF2", Light Metals, 1995, 73-82.
16. Wang J., Li C., Chai D., Zhou Y., Fang B., and Li Q., "Relationship between Aluminium Electrolysis Current Efficiency and Operating Condition in Electrolyte Containing High Concentration of Li and K", Light metals, 2018, 621-626.

17. Dedyukhin A., Apisarov A., Tin'ghaev P., Redkin A., Zaikov Y., "Electrical conductivity of the KF-NaF-AlF_3 molten system at low cryolite ratio with CaF_2 addition", Light metals, 2011, 563-565.
18. Dewing E.W., "Loss of Current Efficiency in Aluminium Electrolysis Cell", Metallurgical Transaction B, 1991, 22B, 177-182.
19. Korenko M., Priscak J., Simko F., "Electrical conductivity of system based on Na_3AlF_6-SiO_2 melt", Chemical papers, 2013, 67 (10), 1350-1354.
20. Korenko M., Vaskova Z., Simko F., Simurda M., Ambrova M., Shi Z., "Electrical conductivity and viscosity of cryolite electrolytes for solar grade silicon (Si-SoG) electrowinning", Trans. Nonferrous Met. Soc. China, 2014, 24, 3944−3948.
21. Padamata S. K., Yasinskiy A. S., Polyakov P. V., "Electrolytes and its additives used in aluminium reduction cell: a review", Metallurgical research and technology, 2019, 116 (4), 410.
22. Glucina M., Hyland M. "Laboratory scale testing of Aluminium Bronze as an Inert anode for Aluminium Electrolysis", Light Metals 2005, 523-528.
23. Tkacheva O., Spangenberger J., Davis B., and Hryn J., Chapter 1.6 "Aluminium Electrolysis in an Inert Anode Cell. Molten Salts Chemistry and Technology", John Wiley & Sons, Ltd, 2014, First Edition, 53–69.
24. Yasinskiy A.S., Polyakov P.V., Voyshel Y.V., Gilmanshina T.R., Padamata S.K., "Sedimentation behaviour of high-temperature concentrated colloidal suspension based on potassium cryolite", Journal of Dispersion Science and Technology, 2018, 39 (10), 1492-1501.
25. Yasinskiy, A., Suzdaltsev, A., Padamata, S.K., Polyakov, P., Zaikov, Yu., "Electrolysis of low–temperature suspensions: an update", Minerals, Metals and Materials Series: Light metals, 2020 (In press).
26. Keller R., Rolseth, S., Thonstad J., "Mass transport considerations for the development of oxygen-evolving anodes in aluminium electrolysis", Electrochimica Acta, 1997, 42 (12): 1809–1817.
27. Yasinskiy A. S., Padamata S. K., Polyakov P. V., Vinogradov O.O., "Anodic process on aluminium bronze in low-temperature cryolite-alumina melts and suspensions", Tsvetnye Metally., 2019, 9, 42-49.
28. Yasinskiy A. S., Padamata S. K., Polyakov P. V., Samoilo A.S., Suzdaltsev A.V., Nikolaev A.Y., "Electrochemical behaviour of Cu-Al oxygen-evolving anodes in low-temperature fluoride melts and suspensions", Minerals, Metals and Materials Series: Light metals, 2020 (In press)
29. Gohar G.A., Manzoor T., Shah A.N., "Investigation of thermal and mechanical properties of Cu-Al alloys with silver addition prepared by powder metallurgy", Journal of Alloys and Compounds, 2018, 735, 802-812.
30. Cao D., Shi Z., Shi D., Xu J., Hu X., Wang Z., "Electrochemical oxidation of Fe-Ni alloys in cryolite-alumina molten salts at high temperature", Journal of Electrochemical Society, 2019, 166 (4), E87-E96.
31. Nikolaev, A. Yu., Suzdaltsev, A.V., Polyakov, P.V., Zaikov, Yu. P., "Cathode process at the electrolysis of KF-AlF_3-Al_2O_3 melts and suspensions", Journal of Electrochemical Society, 2017, 164 (8), H5315-H5321.
32. Ratkje S.K., "Oxy-fluoro aluminate complexes in molten cryolite melts", Electrochimica Acta, 1976, 21, 515–517.
33. Picard G.S., Bouyer F.C., Leroy M., Bertaud Y., Bouvet S., "Structures of oxyfluoroaluminates in molten cryolite-alumina mixtures investigated by DFT-based calculations", Journal of Molecular Structure: THEOCHEM, 1996, 368, 67–80.
34. Cañizares P., García-Gómez J., Fernández de Marcos I., Rodrigo M.A., and Lobato J., "Measurement of Mass-Transfer Coefficients by an Electrochemical Technique", Journal of Chemical Education, 2006, 83 (8), 1204-1207.
35. Yan H., Yang J., Li W., And Chen S., "Alumina Solubility in KF-NaF-AlF_3-Based Low-Temperature Electrolyte", Metallurgical and Materials Transactions B, 2011, 42B, 1065-1070.

36. O. Tkacheva, Yu. Zaikov, A. Apisarov, A. Dedyukhin, A. Redkin, The aluminum oxide solubility in the KF-NaF-AlF_3 melts, Proceedings of the eight Israeli-Russian bi-national workshop 2009 'The optimization of the composition, structure and properties of the metals, oxides, composites, nano- and amorphous materials', Israel, (2009) 175-182.
37. J. D. Weyand, D. H. DeYoung, S. P. Ray, G. P. Tarcy and F. W. Baker, "Inert anodes for aluminium smelting", Contract DE-FC07-80CS40158, Final Report, DOE/CS/40158-20, 1986.
38. D. M. Strachan, 0. H. Koski, L. G. Morgan, R. E. Westerman, R. D. Peterson, N. E. Richards and A. T. Tabereaux, "Results from a 100-hour test of a Cermet anode: materials aspects", Light Metals, 1990, 395-401.